

An agarose hydrogel biomimetic mineralisation model for the regeneration of enamel prism-like tissue

Ying Cao^{†,‡}, May Lei Mei[†], Quan-Li Li^{*‡}, Edward Chin Man Lo[†] and Chun Hung Chu^{*†}

[†]Faculty of Dentistry, The University of Hong Kong, Hong Kong, China

[‡]College of Stomatology, Anhui Medical University, Hefei, China

⁶**KEYWORDS:** Enamel, Mineralisation, Model, Prism, Regeneration, Nano-indentation.

⁸**ABSTRACT:** Laboratory studies have demonstrated that enamel-like mineralised tissue can be regenerated and used to repair enamel loss. This has implications for the management of non-cariou tooth loss due to dental erosion, attrition and abrasion. In this study, we designed a hydrogel biomimetic mineralisation model for the regeneration of enamel-like mineralised tissue with a prismatic structure. The mineralised tissue, which was generated by the model on an etched enamel surface in the presence of 500 ppm fluoride, was analysed with a scanning electron microscope, X-ray diffraction, Fourier transform infrared spectroscopy and the nano-indentation hardness test. The generated tissue had enamel prism-like layers containing well-defined hexagonal hydroxyapatite crystals. The modulus of elasticity and nano-hardness of the regenerated enamel prism-like tissue were similar to those of natural enamel. Thus, the regeneration of enamel using this hydrogel biomimetic mineralisation model is a promising approach for the management of enamel loss.

17 1. INTRODUCTION

¹⁸ Dental enamel is a highly mineralised tissue made up of
¹⁹ approximately 95% substituted hydroxyapatite, 4% water and
²⁰ 1% organic macromolecules.(1) It consists of nanorod-like
²¹ hydroxyapatite (HA) crystals arranged into well-organised
²² micro-architectural units called enamel prisms.(2) Enamel
²³ prisms are an important factor in the remarkable mechanical
²⁴ properties of dental enamel, which protects teeth from fractures
²⁵ and acid attacks.(3) During enamel formation, ameloblasts
²⁶ secrete amelogenin. Amelogenin is approximately 90% organic
²⁷ matrix material. It spontaneously self-assembles into nano-
²⁸ spheres that promote the formation and growth of crystallites,
²⁹ which form a well-organised prism pattern.(4) The
³⁰ hydroxyapatite crystals grow rapidly as the enamel matures
³¹ and the amelogenin degrades into small fractions, resulting in
³² the formation of a highly mineralised tissue with a well-
³³ organised micro-architecture. The ameloblasts undergo
³⁴ apoptosis after the enamel is formed. Enamel is a non-living
³⁵ mineralised tissue that is susceptible to demineralisation by
³⁶ bacterial and chemical acids in unfavourable environments. It
³⁷ is also subject to mechanical damage through attrition or
³⁸ abrasion.(5)

³⁹
⁴⁰ Previous studies have proposed various methods for
⁴¹ regenerating the enamel microstructure and repairing enamel
⁴² defects based on cell-free strategies, including a hydrothermal
⁴³ method using the controlled release of calcium from Ca-
⁴⁴ EDTA,(3) hydrothermal transformation of octacalcium
⁴⁵ phosphate rod to HA nano-rods in the presence of gelatine,(6)
⁴⁶ surfactant supported HA self-assembly,(7) hydrogen peroxide
⁴⁷ containing calcium phosphate paste(8) and an electrolytic
⁴⁸ deposition system at 85°C.(9) However, All of these methods
⁴⁹ are performed under conditions of high temperature, high
⁵⁰ pressure or extremely low acidity. Recently, amelogenin was

⁵¹ used to control enamel remineralisation to form enamel-like HA
⁵² nanorods under physiological conditions.(10,11) However,
⁵³ amelogenin has difficulty in the expression and purification,
⁵⁴ and also very expensive, which limits its clinical application.

⁵⁵
⁵⁶ The initial formation of enamel apatite in nature occurs
⁵⁷ when a unique gel-like organic matrix interacts with metabolic
⁵⁸ and intricate cell activities. The enamel at the secretory or
⁵⁹ matrix formation stage has a gel-like consistency.(12) In that
⁶⁰ gel-like micro-environment, the mode of crystal growth is
⁶¹ different than in aqueous solutions. Busch and his co-workers
⁶² developed a method to mimic the gel-like micro-
⁶³ environment.(13) They used Ca²⁺ and HPO₄²⁻ diffusion in
⁶⁴ gelatine to induce the formation of enamel-like fluorapatite on
⁶⁵ human enamel. The physio-chemical nature of this gel-like
⁶⁶ micro-environment more realistically mimics the unique
⁶⁷ mineralised tissue matrix environment than aqueous
⁶⁸ solutions.(14) However, gelatine is sol at physiological
⁶⁹ temperature which limits its application. Glycerine was added
⁷⁰ to increase the melting temperature of gelatine to 40°C, but this
⁷¹ could be a concern on biosafety when applied in oral
⁷² environment for a long time. Agarose is a natural
⁷³ polysaccharide with good biocompatibility. It has been widely
⁷⁴ used in biomedicine. The temperature of sol-gel translation of
⁷⁵ agarose is at about 60°C which can overcome the limitation of
⁷⁶ gelatine. In this study, we demonstrated that an enamel prisms-
⁷⁷ like structure can be regenerated by an agarose hydrogel
⁷⁸ biomimetic mineralisation model under physiological
⁷⁹ conditions using agarose, without using cell and/or enamel
⁸⁰ protein.

82 2. MATERIALS AND METHODS

⁸³ **2.1. Tooth slices preparation.** This study was approved by
⁸⁴ The University of Hong Kong/Hospital Authority Hong Kong

85 West Cluster Institutional Review Board (IRB UW10-210).
86 Extracted sound human third molars were collected with
87 patients' consent. The teeth were disinfected with 3% sodium
88 hypochlorite and rinsed with phosphate-buffered saline. Tooth
89 slices of 2 mm thickness were prepared perpendicular to the
90 longitudinal axis of each tooth using a low speed diamond saw
91 (IsoMet Low Speed Saw, Buehler, Lake Bluff, Illinois, USA).
92 The slices were polished with silicon carbide papers and then
93 ultrasonically cleaned with deionised water. They were stored
94 in a polyethylene tube at 4°C.

95
96 **2.2. Hydrogels and phosphate solution preparation.**
97 Calcium chloride (CaCl₂) hydrogel was prepared by mixing
98 0.5g agarose powder (BIOWEST Regular Agarose G-10, Gene
99 Company, Origin, Spain), 1.9g CaCl₂ · 2H₂O and 100ml
100 deionised water. An ion-free hydrogel was prepared by
101 dissolving 0.5g agarose powder in 100ml deionised water. Their
102 pH values were adjusted to 6.5 using 0.1 M NaOH and 0.1 M
103 HCl. The mixtures were allowed to swell at 25°C for 30 min
104 before being heated to 100°C. The two hydrogels were kept at
105 60°C after complete dissolution before use. The 0.26M
106 phosphate solution (pH adjusted to 6.5) was prepared by
107 dissolving Na₂HPO₄ in deionised water. Sodium fluoride was
108 added to the phosphate solution to obtain a final concentration
109 of fluoride 500 ppm.

110
111 **2.3. Enamel regeneration in hydrogel biomimetic
112 mineralisation model.** Tooth slices were etched with 37%
113 phosphoric acid for 1 min, rinsed with deionised water and put
114 into polyethylene tubes. The slices were first covered with a 2-
115 mm-thick layer of CaCl₂ hydrogel and then covered with a 2-
116 mm-thick layer of ion-free hydrogel. After gelification, the
117 polyethylene tubes were filled with 10 mL of phosphate
118 solution. A 4-layer (enamel slice, CaCl₂ hydrogel, ion-free
119 hydrogel and phosphate solution) hydrogel biomimetic
120 mineralisation model was then constructed (Figure 1). The
121 polyethylene tubes were sealed and incubated at 37°C. The
122 phosphate solution was replaced every 24 hours and the
123 hydrogels were replaced every 48 hours. Before replacing the
124 hydrogels, the tooth slices were cleaned ultrasonically with
125 deionised water for 20 sec. They were taken out for examination
126 after incubation for 2, 4 and 6 days.

127
128 **2.4. Assessment of regenerated enamel and hydrogels.** The
129 morphology of the precipitates were characterised by field
130 emission scanning electron microscope (SEM) and atomic force
131 microscope (AFM). For SEM, the slices were sputter-coated
132 with gold for observation (S4800, Hitachi High Technologies
133 America, Inc., Dallas, USA). AFM analysed using a Tapping
134 Model Etched Silicon Probe (Dimension Edge, Bruker,
135 California, USA). The phase composition, structure and
136 orientation of the regenerated tissue were confirmed by X-Ray
137 Diffraction (XRD) (X'Pert PRO, Philips, Almelo, Netherlands).
138 Fourier transform infrared (FTIR) spectra of the regenerated
139 tissue were collected by means of a Multiscope FTIR
140 spectrometer (Nicolet 8700, Thermo Scientific Instrument Co.
141 Friars Drive Hudson, NH, USA). The replaced agarose
142 hydrogels were dehydrated with ethanol and then dried in a
143 critical evaporator for SEM and transmission electron
144 microscopy (TEM) evaluation (Tecnai G2 20, FEI Co.,
145 Eindhoven, Netherlands). Selected area electron diffraction

146 (SAED) was used to identify the minerals structures in the
147 hydrogel.

148
149 **2.5. Evaluation of mechanical properties.** The surface of
150 the tooth slices was divided into three sections. The first section
151 was covered with acid-resistant and hydrophobic nail vanish
152 (Revlon, New York, USA) (untreated enamel). The nail vanish
153 was used to protect the enamel surface from treatment such as
154 acid etching and subsequent remineralisation, so that they can
155 be used as control for comparison. The second section was
156 covered with nail vanish after being etched with 37%
157 phosphoric acid for 1 min (etched enamel). The third section
158 was etched with 37% phosphoric acid for 1 min (this was the
159 area where regenerated mineralised tissue formed after
160 biomimetic mineralisation). Three tooth slices were incubated
161 in the hydrogel biomimetic mineralisation model for 6 days.
162 They were then immersed in acetone to remove the nail vanish
163 to expose the three areas of untreated enamel, acid-etched
164 enamel, and regeneration enamel). Subsequently, they were
165 cleaned ultrasonically with deionised water for 20 sec and
166 stored in deionised water at 23°C. The mechanical properties,
167 namely the elastic modulus and nano-hardness, of the
168 regenerated mineralised tissue on the third section were
169 compared to the properties of the untreated enamel and etched
170 enamel on the same tooth slices surface. A nano-indentation test
171 using the Berkovich tip was used to analyse the elastic modulus
172 and nano-hardness of each section (G200, Agilent Technologies,
173 CA, USA). The tip was calibrated with a fused-silica sample
174 prior to evaluation.

175
176 The nano-indentation test consisted of three segments: the
177 loading segment, the peak load holding segment and the
178 unloading segment. The times for both loading and unloading
179 were 15 sec. The holding time was 10 sec. Sixteen indentations
180 were made on each section of three tooth slices. Thus a total of
181 144 indentations were performed on 9 sections from 3 tooth slices
182 The maximum force applied during loading and unloading was
183 10 gf (0.098 N). The applied load forces and the depth of
184 penetration into the samples during the indentation were
185 continuously monitored by computer. The data were recorded
186 and processed by Testworks 4 software (MTS Systems
187 Corporation, Eden Prairie, MN, USA), which calculated the
188 elastic modulus and nano-hardness and presented them as force-
189 displacement curves. The differences in the elastic modulus and
190 nano-hardness among the three sections of tooth slices were
191 assessed with a two-way ANOVA. A 5% significance cut-off
192 level was used for the statistical analysis. An optical microscope
193 and SEM were used to examine the residual indent impressions.

194
195 **3. RESULTS**

196 **3. 1. Assessment of regenerated enamel and hydrogels.**
197 Rod crystals were found on the enamel surfaces after 2 days of
198 incubation in the hydrogel biomimetic mineralisation model
199 (Figure 2a). The rod crystals extended out the enamel prism
200 surface after 2 day incubation. The c-axial orientation of these
201 crystals was perpendicular to the enamel prism (Figure 2b). The
202 newly precipitated rod crystals on the surface were not densely
203 packed and were relatively separated. The spaces between the
204 rod crystals were filled with hydrogel matrix (Figure 2c). The
205 examination of the slices in cross-section found that the rod
206 crystals precipitated from the enamel surface (Figure 2d).

207 Notably, the rod crystals were not haphazardly distributed and
208 their orientation was almost perpendicular to the underlying
209 enamel. These rod crystals fused with those in the underlying
210 enamel. The lengths along *c*-axis of the crystals were shorter
211 than that of the following growth crystals at 6 days.

212
213 Well-defined and orderly distributed rod crystals with a
214 typical apatite hexagonal structure were found after 4 days of
215 incubation in the model (Figure 3a). The hexagonal rod crystals
216 were approximately 150 nm in diameter and 2 μm in length.
217 They were densely packed along the *c*-axis, pushing the rod
218 crystals parallel to each other. **Certain rod crystals self-**
219 **assemble together to form the rudiment of enamel prism-like**
220 **bundles (Figure 3b Oval).** There was a negligible amount of
221 hydrogel matrix left in the spaces between them (Figure 3b
222 Arrow). The crystallographic *c*-axis of these rod crystals shared
223 the same orientation and they were perpendicular to the
224 underlying enamel surface (Figure 3c, d).

225
226 The regenerated crystals on the enamel surface formed a
227 homogenous and dense layer of mineralised tissue after 6 days
228 of incubation (Figure 4a). The strong attraction between
229 adjacent rods caused them to fuse together to form an extensive
230 layer of well-aligned crystals on the enamel surface (Figure 4b).
231 These regenerated crystals had a tendency to spontaneously
232 aggregate, side by side, to form bundles of enamel prism-like
233 structures along the *c*-axis of the rods (Figure 4c, 4d). The
234 bundled crystals had a width of approximately 1-2 μm and were
235 very similar in appearance to the natural enamel surface. These
236 bundled crystals consisted of agglomerative nano-crystals
237 (Figure 4c). They assembled in a well-organised manner and
238 were densely packed to form a homogeneous layer of
239 mineralised tissue on the enamel surface (Figure 4d). Generally,
240 the long axes of the crystals were radially perpendicular to the
241 underlying enamel surface. The thickness of the enamel prism-
242 like surface was approximately 3.5 μm after 6 days (Figure 4e).
243 The interface between the regenerated tissue and the underlying
244 enamel showed a tight agglomeration and fusion (Figure 4f).
245 There was hardly any hydrogel matrix between the crystal
246 bundles.

247
248 **Figure 5 showed the surface variation in the spatial direction**
249 **of crystals in 3D AFM images of acid-etched enamel and the**
250 **regenerated enamel. The enamel prisms with parallel bundles of**
251 **hydroxyapatite crystals were observed after the enamel slices**
252 **acid-etched for 1 min (Figure 5a). The newly precipitated**
253 **crystals stuck out from the enamel surface. They were relatively**
254 **separated and not densely packed on the enamel surfaces after**
255 **2 days of incubation in the hydrogel biomimetic mineralisation**
256 **model (Figure 5b). This made the enamel surface rough. The**
257 **paralleled crystals densely packed along the *c*-axis and form the**
258 **rudiment of enamel prism-like bundles after 4 days (Figure 5c).**
259 **The bundles with the enamel prism-like structure were formed**
260 **after 6 days (Figure 5d) which was similar to sound enamel**
261 **(Figure 5a). AFM findings corresponded well to the SEM**
262 **results.**

263
264 **In this hydrogel biomimetic mineralisation model,**
265 **numerous polymer (agarose fibre)-mineral complex globules**
266 **were found in the replaced CaCl_2 hydrogel adjacent to the**
267 **enamel surface after 2 days (Figure 6a). These globules were**

268 **formed by the coalescence of small nano-spheres (Figure 6b and**
269 **6c). The blurred ring patterns that formed instead of the sharp**
270 **and clear arc-shaped patterns in the SAED of the globules**
271 **suggested an amorphous structure or a very low crystallization**
272 **(Figure 6d). Very few globules were found in the replaced ion-**
273 **free hydrogel near the phosphate solution (Figure 6e and 6f).**

274
275 **The XRD patterns of the regenerated crystals after 2, 4 and**
276 **6 days of incubation are shown in Figure 7a. The diffraction**
277 **peaks (002) at $2\theta=25.8$, (211) at $2\theta=31.8$, (112) at $2\theta=32.2$ and**
278 **(300) at $2\theta=32.8$ corresponded well to the peaks for fluoridated**
279 **hydroxyapatite (HA) (JCPDS No. 09-0432),(10) suggesting**
280 **that the crystals were fluoridated HA.(15) The sharp and intense**
281 **002 peak indicated that the crystals were well crystallised and**
282 **oriented along their *c*-axis; these results were consistent with**
283 **the observations in the SEM images (Figure 5). After 6 days of**
284 **incubation, the XRD pattern showed that the diffraction peaks**
285 **around 2θ of 32° were split and clear, which implied good**
286 **crystallinity of fluoridated HA. Moreover, the (300) diffraction**
287 **peak was broad, indicating a lattice strain (microstrain) caused**
288 **by the shift of the nano-crystals from their normal positions. In**
289 **addition, the peak around 2θ of 44.6° was very sharp, perhaps**
290 **due to the microstrain caused by the agglomerative individual**
291 **nano-crystals.(16) These results were consistent with the SEM**
292 **observation (Figure 4). The FTIR analysis also confirmed the**
293 **formation of a typical apatite structure over time. The FTIR**
294 **spectra shown in Figure 7b demonstrated the presence of**
295 **phosphate groups on the etched enamel surfaces. The splitting**
296 **$\text{PO}_4 \nu_4$ band was present in the region of 660 and 520 cm^{-1} . A**
297 **well-defined and sharp band was observed in the HA. The split**
298 **$\text{PO}_4 \nu_3$ band at about 1037 and 1117 cm^{-1} came from HA**
299 **crystals.(17) There was no -OH group specific peaks at $1,571$**
300 **cm^{-1} , indicating that -OH group might be replaced by F group**
301 **to form fluoridated HA.(15) It should be noted that some**
302 **information might be lost due to the reflection mode of FTIR,**
303 **which is difficult to distinguish between FA and HA. It should**
304 **be analysed together with other methods, such as XRD and**
305 **morphological change of the crystals.**

306
307 **3. 2. Evaluation of mechanical properties.** Figure 8
308 illustrates the typical loading-unloading curves (8a) and the
309 calculated elastic modulus and nano-hardness (8b) of the
310 untreated, regenerated and etched enamel. The mean ($\pm\text{SD}$)
311 elastic modulus and mean nano-hardness of the enamel after
312 acid etching were significantly reduced from $90.31\pm 7.63 \text{ GPa}$
313 and $4.28\pm 0.53 \text{ GPa}$, respectively (untreated enamel) to
314 $58.05\pm 9.93 \text{ GPa}$ and $1.03\pm 0.31 \text{ GPa}$ (etched enamel),
315 respectively. After 6-day incubation, the mean elastic modulus
316 and mean nano-hardness of the enamel were significantly
317 increased to $89.46\pm 11.82 \text{ GPa}$ and $3.04\pm 0.75 \text{ GPa}$, respectively
318 (regenerated enamel). There were no significant differences in
319 elastic modulus or nano-hardness between the regenerated and
320 untreated enamel.

321
322 **Figure 9a shows an optical microscope image of a**
323 **regenerated enamel surface with 16 nano-indentations. The**
324 **nano-indentation impressions form a triangular pyramid. No**
325 **cracks were found around the indentations. The impression area**
326 **on the surface of the regenerated enamel (Figure 9c) was similar**
327 **to that on the untreated enamel (Figure 9b) and both were**
328 **smaller than on the etched enamel (Figure 9d).**

330 4. DISCUSSION

331 **4.1. An agarose hydrogel biomimetic mineralisation**
 332 **model.** The transportation of ions through the organic matrix
 333 and the interactions between the ions and the organic matrix are
 334 crucial in the regulation of the enamel mineralisation
 335 process.(18) The process is mediated by enamel matrix proteins
 336 (mainly amelogenin and enamelin) and can be divided into
 337 several phases.(18) The proposed molecular mechanisms for
 338 the functions of enamel matrix proteins in enamel
 339 mineralisation include i) the prevention of the crystal fusion of
 340 pre-mature crystal,(19) ii) the control of crystal morphology
 341 and subsequent elongation(20) and iii) the control of the
 342 nucleation and growth of the crystals.(21)

343

344 At the secretion stage, the enamel organic matrix has a gel-
 345 like consistency, which results in enamel apatite formation
 346 taking place under a unique gel-like organic matrix
 347 environment rather than in aqueous solutions. The mode of
 348 crystal growth in a gel-like micro-environment is different than
 349 in aqueous solutions. During enamel formation, Ca^{2+} and PO_4^{3-}
 350 ions are transported from the layer of ameloblasts into the
 351 enamel matrix where the mineralisation takes place. In the
 352 process of enamel matrix secretion and calcification,
 353 ameloblasts withdraw from the mineralising area. There is a
 354 unidirectional supply of Ca^{2+} and PO_4^{3-} and this unidirectional
 355 ion supply is thought to play a key role in enamel crystal growth
 356 and orientation.(22)

357

358 In the present study, agarose hydrogel was used to mimic
 359 the gel-like organic matrix environment to induce enamel-like
 360 tissue regeneration. A unidirectional supply of Ca^{2+} and PO_4^{3-}
 361 were achieved in this model. We found no precipitates of
 362 calcium phosphate in the ion-free hydrogel (Figure 6e and 6f).
 363 This suggested that there was little diffusion of calcium ions
 364 from the CaCl_2 hydrogel to the ion-free hydrogel. On the
 365 contrary, the calcium ions accumulated in the CaCl_2 hydrogel
 366 layer. Meanwhile, the phosphate ions diffused from the PO_4^{3-}
 367 solution through the ion-free hydrogel into the CaCl_2 hydrogel
 368 and enamel surface. Furthermore, the mineralizing precursor of
 369 agarose fibre-mineral complex was formed. The organic matrix
 370 can prevent pre-mature crystal-crystal fusion, control the
 371 subsequent phase transformations, and control the nucleation
 372 and growth of the crystals. In our model, the hydrogel stabilised
 373 the mineral precursors and prevented them from transforming
 374 into crystal (Figure 6). The mineral precursors in the hydrogel
 375 were very small and less readily crystallised. This may have
 376 contributed to the strong attractive interaction between the
 377 agarose polymer and the inorganic surface, which can in turn
 378 arrest nucleation and change the shape and size of the primary
 379 clusters. The mechanism of the crystal growth will be discussed
 380 below.

381

382 Agarose is a natural polysaccharide and consists of a linear
 383 polymer with repeating units of D-galactose and 3, 6-anhydro
 384 L-galactose. It is low-cost and biocompatible, and has been
 385 widely used in biomedicine. Comparing to the glycerine-rich
 386 gelatine hydrogel model(13), the temperature of sol-gel
 387 transition of agarose is higher than the physiological
 388 temperature at which gelatine melts. The mechanical strength
 389 of the agarose is higher than gelatine, safer than the glycerine-

390 rich gelatine hydrogel, and with no ethical concerns. The
 391 strength and consistency of the hydrogel can be adjusted by
 392 varying the concentration and molecular weight of the agarose.
 393 These make it easy to transfer to clinical use. On the other hand,
 394 the mechanism of regeneration of enamel-like tissue is also
 395 different between the gelatine model and our agarose model. In
 396 the gelatine model, the amino groups of gelatinous polypeptide
 397 can form salt-like bonds to phosphate groups on the apatite
 398 surface, and thus to induce the regeneration of enamel-like
 399 minerals.(13) The gelatine hydrogel entrapped phosphate
 400 groups in the hydrogel, which result in their method as enamel
 401 surface-phosphate ions hydrogel. However, in our model,
 402 calcium ions were entrapped in the hydrogel, which result in the
 403 method as enamel surface-calcium ions hydrogel. If we
 404 assembled the hydrogel as enamel surface-phosphate ions
 405 hydrogel, no enamel prism-like tissue could be regenerated in
 406 our study. Fan et al developed an agarose- amelogenin hydrogel
 407 model to regenerate the enamel-like tissue.(23) In their model,
 408 agarose was used as a releasing agent to investigate the function
 409 of amelogenin in the remineralization of early enamel caries.
 410 Although the agarose hydrogel containing calcium and
 411 phosphate without amelogenin was used as the control group,
 412 the different concentration of the inorganic ions and the
 413 different diffusion mode gave different results between our
 414 study and theirs. Moreover, in the absence of amelogenin, they
 415 did not show the regeneration of enamel-like structure. The aim
 416 and function of agarose use, and the results are different
 417 between our study and theirs. Ruan et al developed an
 418 amelogenin-containing chitosan hydrogel for enamel
 419 reconstruction through amelogenin supermolecular assembly,
 420 stabilizing Ca-P clusters and guiding their arrangement into
 421 linear chains.(11) These amelogenin Ca-P composite chains
 422 further fused with enamel crystals and eventually evolved into
 423 enamel-like crystals, anchored to the natural enamel substrate
 424 through a cluster growth process. Both Fan et al's and Ruan et
 425 al's model used amelogenin, but we used an agarose model with
 426 no amelogenin to regenerate enamel-like tissue. Our model is
 427 simple, low cost, biocompatible, and can be transferred
 428 straightforwardly to clinic use. The mechanism need further
 429 study. It may contribute to its agarose molecules, concentration
 430 of hydrogel, and concentration of calcium, phosphate, and
 431 fluoride.

432

433 **4.2. The mechanism of growth of the enamel prism-like**
 434 **crystals.** Classical crystallization pathway is thermodynamic
 435 process where ion-mediated crystallization proceeds via a one-
 436 step route to the final mineral phase.(24) Non-classical
 437 crystallization pathway is a kinetic process where
 438 crystallization proceeds by a sequential process involving
 439 structural and compositional modifications of amorphous
 440 precursors and crystalline intermediates. Crystallization often
 441 involves an initial amorphous phase (such as ACP) that may be
 442 nonstoichiometric, hydrated, and susceptible to rapid phase
 443 transformation.(25) In biology, a biomineralisation process is
 444 an organic matrix particle-mediated non-classical
 445 crystallisation pathway.(26) The organic matrix controls the
 446 mineral crystallites through the molecular interaction between
 447 the polymer and minerals with a sequestering mechanism.(27)
 448 The amorphous primary particles that are formed by ion or
 449 cluster binding at the organic surface can undergo coupled

450 matrix-mediated mesophase transformations resulting in
451 oriented crystallisation with iso-oriented mosaic textures.(24)

452

453 Fluoride has an effect on crystal growth during enamel
454 mineralisation.(10) In the pilot experiment of this study, well-
455 defined rod-like crystals were formed when 500ppm fluoride
456 was added into the phosphate solution. Ribbon-like crystals
457 were observed when the fluoride concentration was reduced to
458 100ppm and only plate-like crystals were found on the enamel
459 surface in the absence of fluoride. (Figure S1, S2 in the
460 Supporting Information).

461

462 The agarose hydrogel in our model functioned as an organic
463 matrix to control the agarose fibre-nano ACP complex
464 precursors (Figure 6). There was strong attractive interaction
465 between abundant hydroxyl OH groups of agarose molecules
466 and Ca^{2+} . This interaction could arrest nucleation and also
467 change the shape and size of the primary mineral clusters when
468 phosphate ions diffusing into the CaCl_2 agarose hydrogel layer.
469 The ACP nanoparticles coalesced and aggregated consisting of
470 inorganic cores surrounded by an organic component (Figure
471 6b). In this way, stabilised nano-ACP or low crystallisation HA
472 with anchored organic ligands was produced in the hydrogel
473 matrix (Figure 6). This corroborated with the observation that
474 there were little mineral complex formed in the layer of ion-free
475 hydrogel (Figure 6e, 6f). Furthermore, the agarose hydrogel
476 acted as a reservoir to replenish mineral precursors and as a
477 dynamic interface to transport the mineral precursors to the
478 enamel surface for the mineral mesocrystal transformation
479 (Figure 10a). With the consistent diffusion of PO_4^{3-} and F into
480 the hydrogel, the metastable ACP nanoparticles kinetically
481 nucleated on the lattice of the enamel HA crystals. The matrix-
482 mediated crystal growth processed by mesophase
483 transformation and aggregation of preformed crystalline
484 building blocks (a mesoscale assembly process, Figure 10b, 10c)
485 resulting in oriented fluoridated HA crystallisation, and creating
486 single crystals with iso-oriented mosaic textures (Figure 4d,
487 10d).

488

489 In this study, the regeneration of enamel prism-like tissue
490 was monitored over 6 days of incubation. The mineral precursor
491 nucleated on the enamel surface by heterogeneous nucleation
492 after 2 days. It grew along its *c*-axis extension. The resultant
493 crystals were perpendicular to the enamel prism surface.
494 Because of the different orientations of the enamel prisms and
495 the nuclei sites, the fluoridated HA oriented disorderly.
496 However, the fluoridated HA crystals were perpendicular to the
497 enamel prism surface where they nucleated. The fluoridated HA
498 crystals were unevenly distributed on the enamel surface. The
499 size of the initial grown crystals in *c*-axis was shorter than the
500 following grown crystals after 4 and 6 days of incubation
501 (Figure 3, 4). Moreover, the nuclei sites were relatively apart,
502 and the hydrogel matrix involved in the nuclei sites. This could
503 provide more space for fluoridated HA crystal growth. As a
504 result, the diameter of the crystals after 2 days (Figure 2c) was
505 larger than the crystals after 4 and 6 days (Figure 3, 4). This
506 finding also corroborated that the involvement of agarose
507 hydrogel in controlling the crystal growth. As more nuclei sites
508 were formed with the progress of the crystal growth, and the
509 amount of agarose hydrogel was gradually reduced. The
510 agarose hydrogel 'draw back' from the mineralizing areas

511 (Figure 3, 4). This phenomenon was similar to the natural
512 enamel formation where enamel proteins degraded resulting in
513 enamel crystal maturing to form prismatic structure. Therefore,
514 the well-defined hexagonal crystals were evenly distributed on
515 the enamel surface after 4 days (Figure 3). The crystals grew
516 along the *c*-axis and densely packed. This mode of crystal
517 growth forced the rod-like crystals to progressively align
518 parallel to each other. The long, large hexagonal crystal
519 probably acted as a primary crystal (seed crystal) enabling the
520 short nanorods to fuse and align parallel to the primary crystal
521 surface and formed crystal bundles. However, the nuclei sites
522 were still relatively apart at 4 days, and most of the crystals were
523 still immature intermediates during the crystal self-assembly or
524 phase transformation. Thus, the morphology of these crystals
525 was different from natural enamel crystal. However, certain rod
526 crystals self-assemble together to form the rudiment of enamel
527 prism-like bundles (Figure 3b Oval). With the crystal growth
528 and assembly, enamel prism-like structure was observed after 6
529 days (Fig.4). The cross-sections of the enamel slices revealed
530 formation of a layer of highly mineralised tissue, which
531 comprised of parallel-oriented and densely packed
532 homogeneous crystals. The mechanism of enamel prism-like
533 tissue assembly is shown in Figure 10 which was based on the
534 SEM observations in our study and referring to mechanism of
535 the non-classical crystallization pathway.(24)

536

537 4.3. Mechanical properties of the regeneration tissue.

538 The nano-indentation test was used to compare the mechanical
539 properties of the regenerated enamel surface with the untreated
540 and etched enamel surfaces. The nano-indentation test is a
541 useful tool for studying mechanical properties at a nano-
542 scale.(28) This depth-sensing technique allows the indentation
543 of minute areas of a few square micrometres, so that the elastic
544 modulus and hardness of small volumes of enamel can be
545 measured.(29) The elastic modulus and nano-hardness obtained
546 from this test should be reasonably acceptable, as no cracks
547 were found around the indentations. It is important to note that
548 the calculation of elastic modulus is based on the unloading
549 curve. The nano-indentation method is therefore applicable to
550 the study of linear, isotropic materials. Enamel consists of
551 mainly apatite crystals and is an orthotropic material. Therefore,
552 errors could arise if there is a "pile-up" or "sink-in" of the
553 enamel surface on the edges of the indent during the indentation
554 process.

555

556 The elastic modulus (90 GPa) and nano-hardness of the
557 untreated enamel (4.3 GPa) were comparable to the results
558 reported by Habelitz and his co-workers(30) (elastic modulus:
559 88 GPa, nano-hardness 4.3 GPa). To minimise the variations of
560 elastic modulus and hardness caused by the different
561 orientations of the enamel prism, the mechanical tests were
562 performed on the untreated, regenerated and etched enamel
563 from the same slices. The elastic modulus (89.5 ± 11.82 GPa)
564 and nano-hardness (3.04 ± 0.75 GPa) of the regenerated tissue
565 on the enamel surface after 6 days of incubation was
566 comparable to those of the untreated enamel surface. The
567 mechanical examination demonstrated that the enamel prism-
568 like layer was characterised by similar mechanical properties as
569 the untreated enamel, probably due to their similar
570 microstructures. Similar results were also reported by Busch et
571 al.(13)

572

573 Wei used fluorapatite cement pastes to fill enamel defects.
574 However, the setting time is very long and at the initial setting
575 stage it is easily washed away by the saliva. Furthermore the
576 fluorapatite crystals in the cement are haphazardly arranged and
577 different from the enamel structure.(15) Many researchers
578 prefer using biomimetic mineralisation to regenerate prsim-like
579 enamel tissue. This study demonstrated that enamel prism-like
580 tissue can be regenerated in a hydrogel biomimetic
581 mineralisation model. Compared to non-hydrogel solution
582 studies, the physio-chemical nature of this enamel regeneration
583 process vividly mimics the unique mineralised tissue matrix
584 environment.(14) It is noteworthy that this model only mimics
585 the gel-like environment in which the initial formation of
586 enamel apatite occurs. Although it is a simplified model, it
587 provides a basis for future research on enamel regeneration.
588 Further studies should add an organic matrix, such as enamel
589 proteins, to the hydrogel biomimetic mineralisation model to
590 mimic the enamel matrix. On the other hand, this biomimetic
591 mineralisation model can be transferred for future clinical
592 applications such as treatment of erosive wear caused by acidic
593 food and inappropriate brushing habit. The CaCl_2 agarose
594 hydrogel, ion-free agarose hydrogel, and phosphate agarose
595 hydrogel can be made commercially. They can be overlapped
596 layer-by-layer to form a sandwich structure inside a tray which
597 the patient will wear overnight. Furthermore, the saliva
598 containing calcium and phosphate ions, and also F-containing
599 mouthwash can be used as the supplement of mineral ions for
600 the mineralisation.

601

602 5. CONCLUSIONS

603 A hydrogel biomimetic mineralisation model to regenerate
604 enamel prism-like tissue was designed. The hydrogel regulated
605 the habit, size and mineral phase of the growing crystals through
606 cooperative interactions with calcium, phosphate and fluoride
607 ions. The regenerated apatite crystals were found to be highly
608 oriented along the *c*-axis, with good crystallinity. The present
609 study provides an important basis for future attempts to develop
610 enamel prism-like material. Hopefully, such material could be
611 used as an alternative treatment in clinical dentistry and other
612 biomedical or industrial applications.

613

614

615

616

617

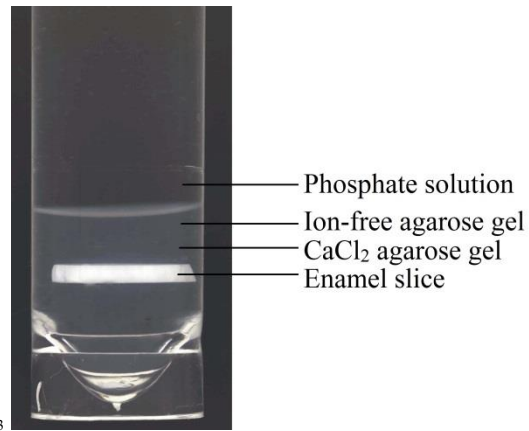
618

619

620

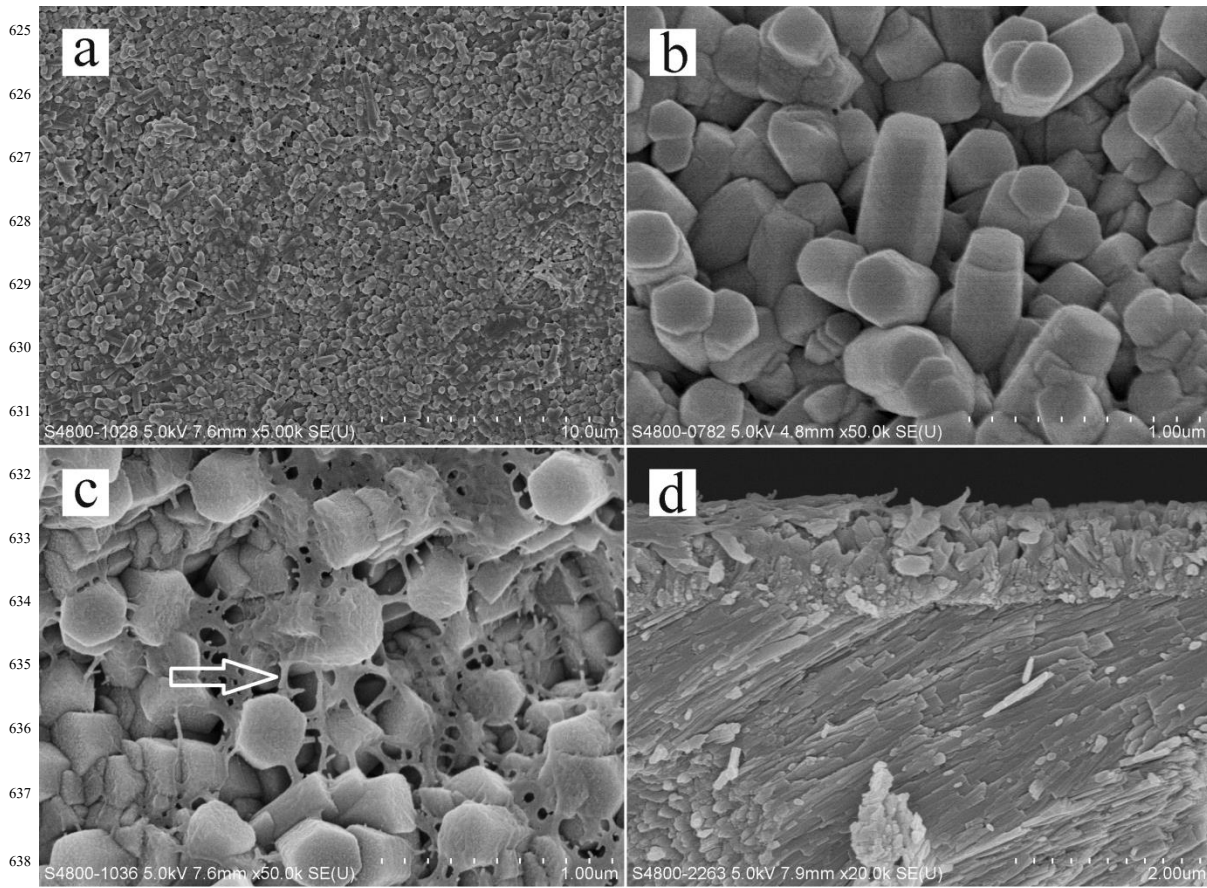
621

622 FIGURES

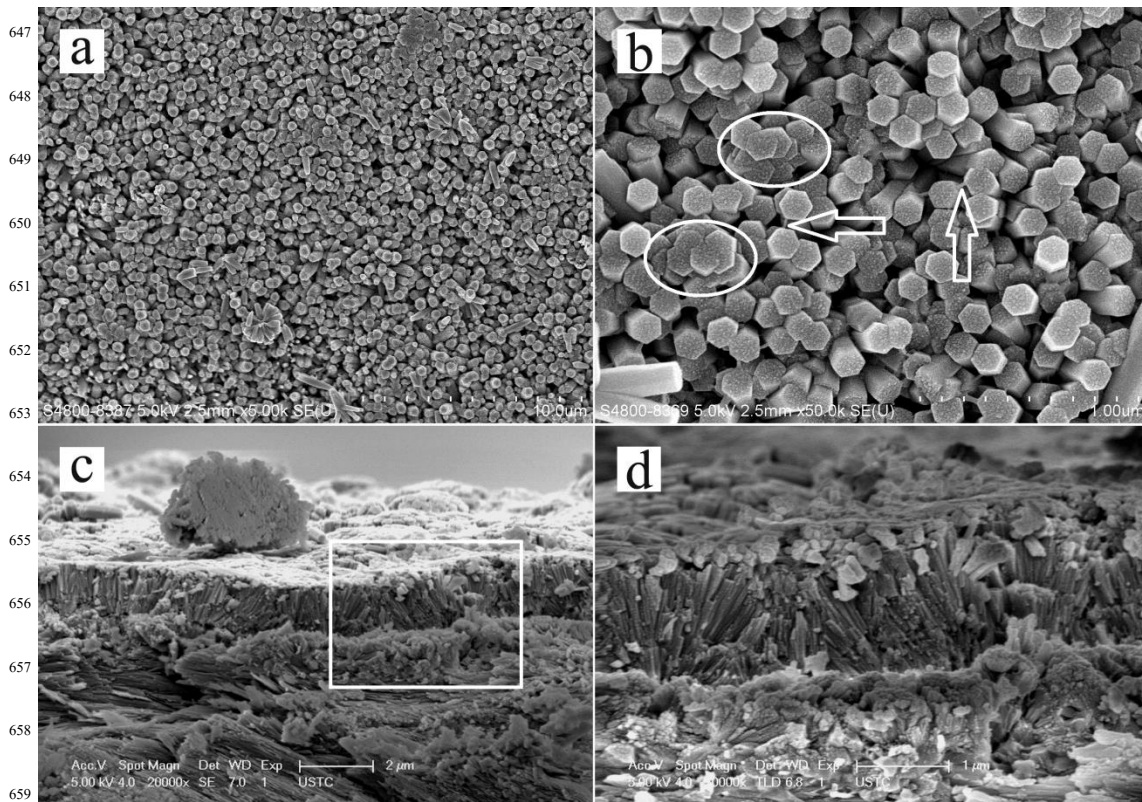


623

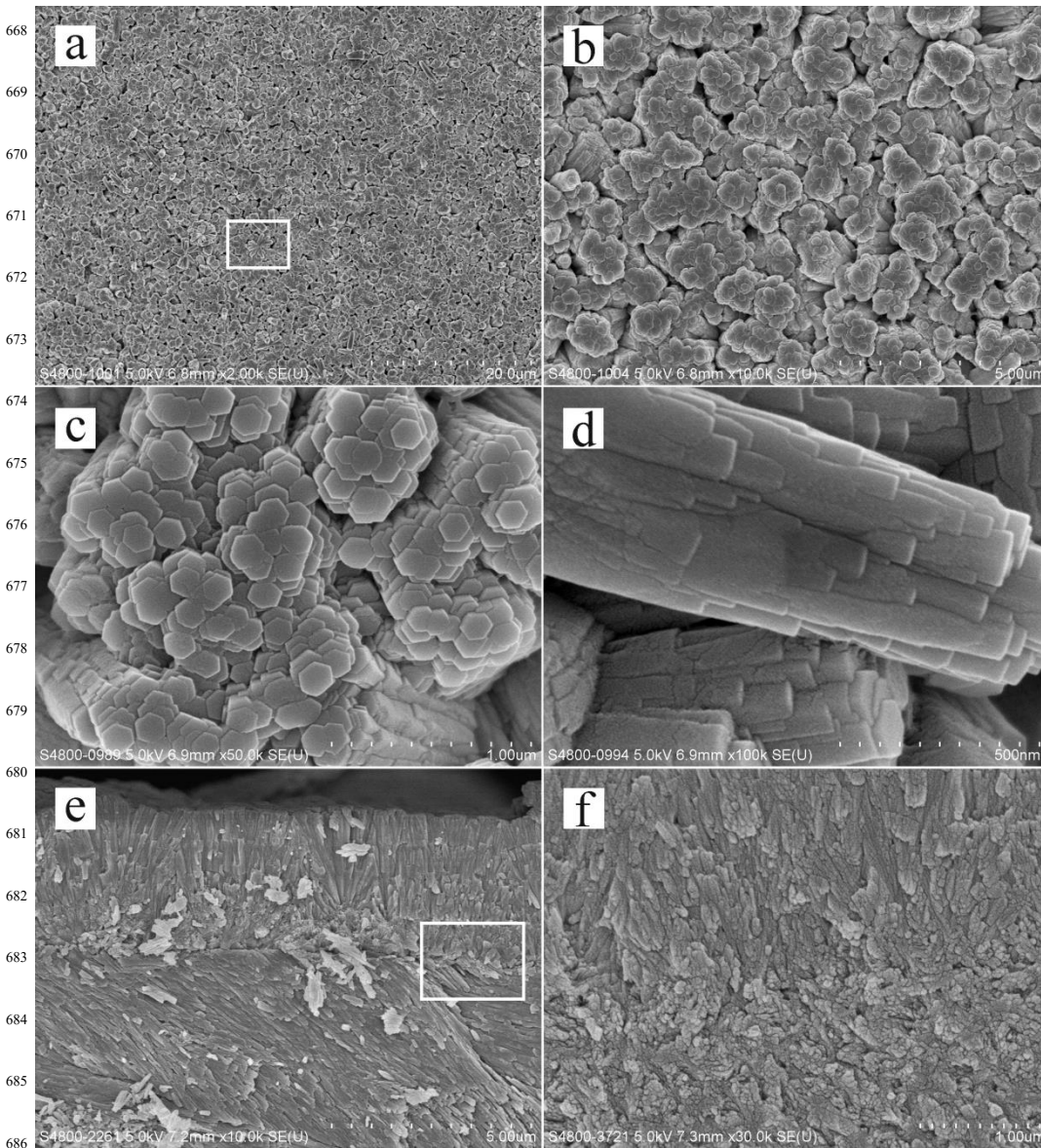
624 Figure 1. The four-layer hydrogel mineralisation model.



639 **Figure 2.** SEM micrographs of the regenerated mineralised
640 tissue after 2 days. (a) Rod-like crystals regenerated on the
641 enamel surface after 2 days. (b) Magnified micrograph of (a)
642 to show that rod-like crystals grew along the *c*-axis. (c)
643 Magnified micrograph of (a) to show the crystals and the
644 hydrogel matrix (Arrow). (d) Cross-sectional view of the
645 regenerated mineralised tissue to show the crystal orientation
646 and prototype of the enamel prism-like structure.

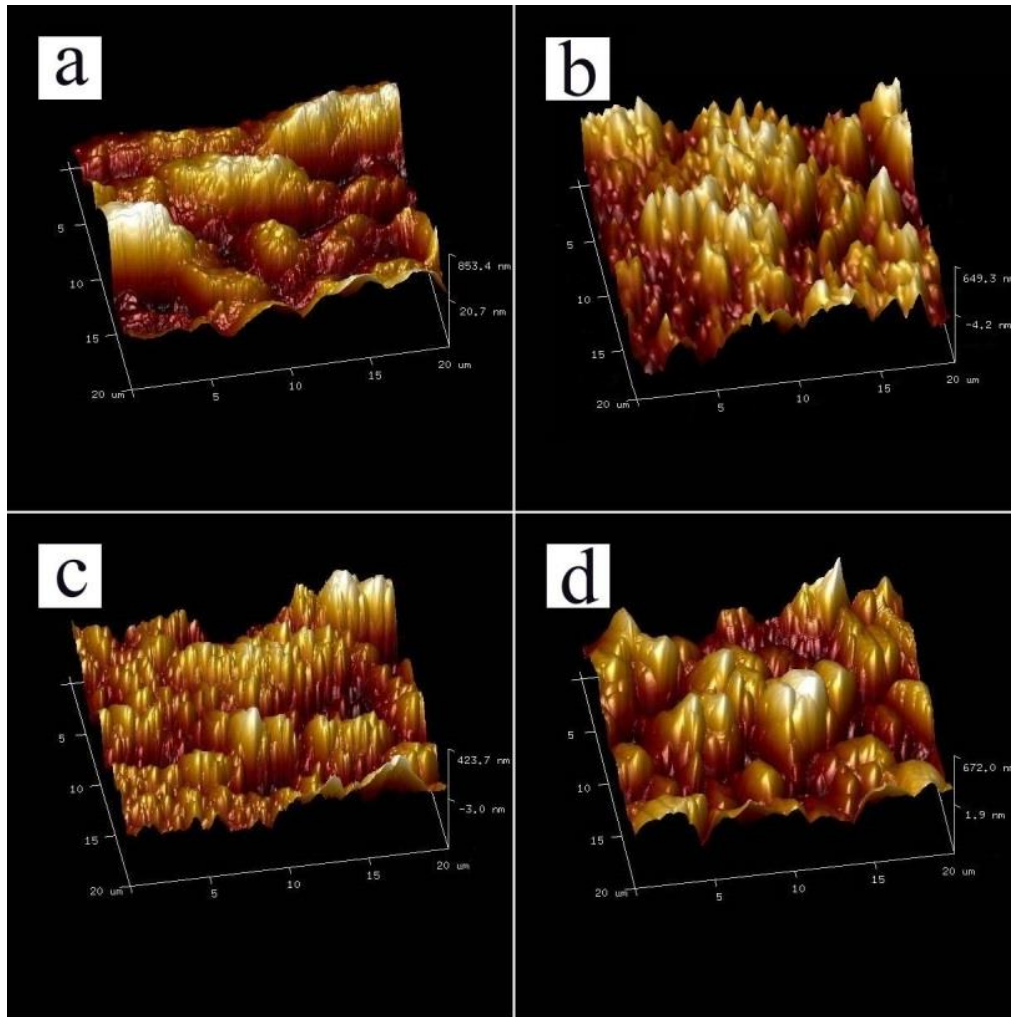


660 **Figure 3.** SEM micrographs of the regenerated mineralised
 661 tissue after 4 days. (a) Rod-like crystals with a typical apatite
 662 hexagonal structure regenerated on the enamel surface. (b)
 663 Magnified micrograph of (a) to show the paralleled crystals,
 664 the rudiment of the enamel prism-like bundles (Oval) and the
 665 hydrogel matrix (Arrow). (c) Cross-sectional view of (a). (d)
 666 Magnified micrograph of the rectangular area of (c).

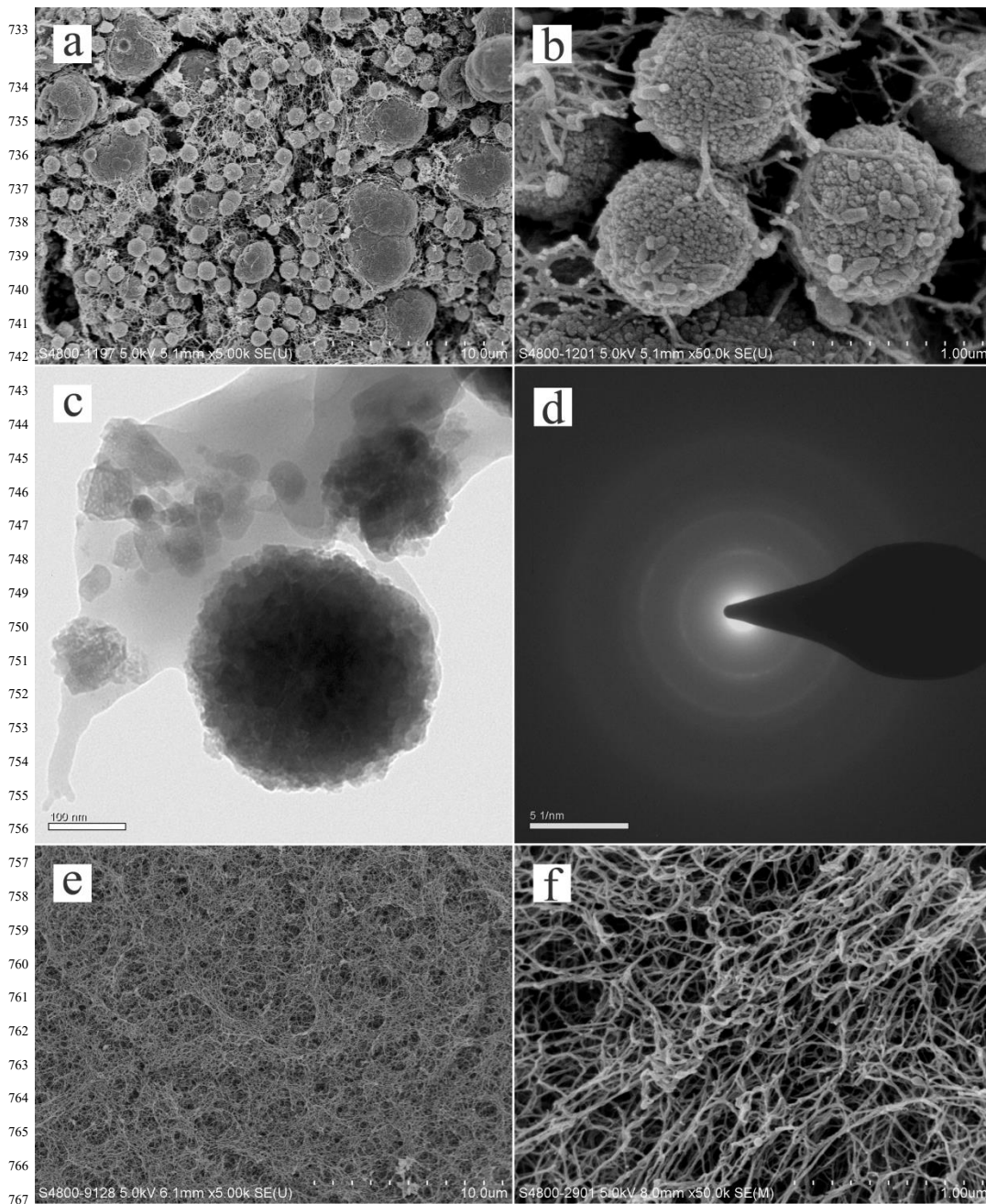


687 **Figure 4.** SEM micrographs of the regenerated mineralised
 688 tissue after 6 days. (a) Mineralised tissue with enamel prism-
 689 like crystals regenerated on the enamel. (b) Magnified
 690 micrograph of (a) to show the paralleled bundles. (c)
 691 Magnified micrograph of (a) to show the agglomerative
 692 hexagonal crystals. (d) Magnified micrograph of the
 693 rectangular area of (a) to show the side view of the crystal
 694 bundle. (e) Cross-sectional view of (a) to show that the
 695 regeneration layer was perpendicular to the underlying
 696 enamel. (f) Magnified micrograph of the rectangular area of
 697 (e) to show the interface between the regeneration tissue and
 698 the underlying enamel.

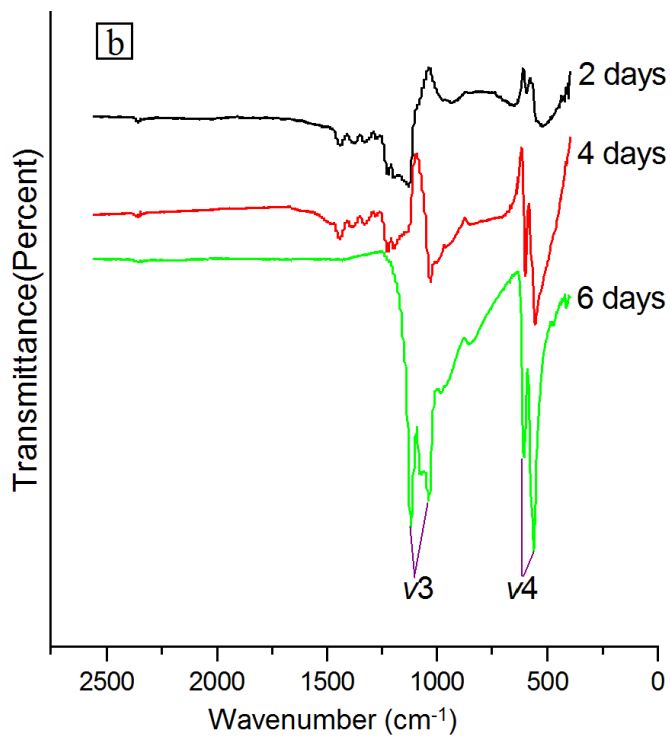
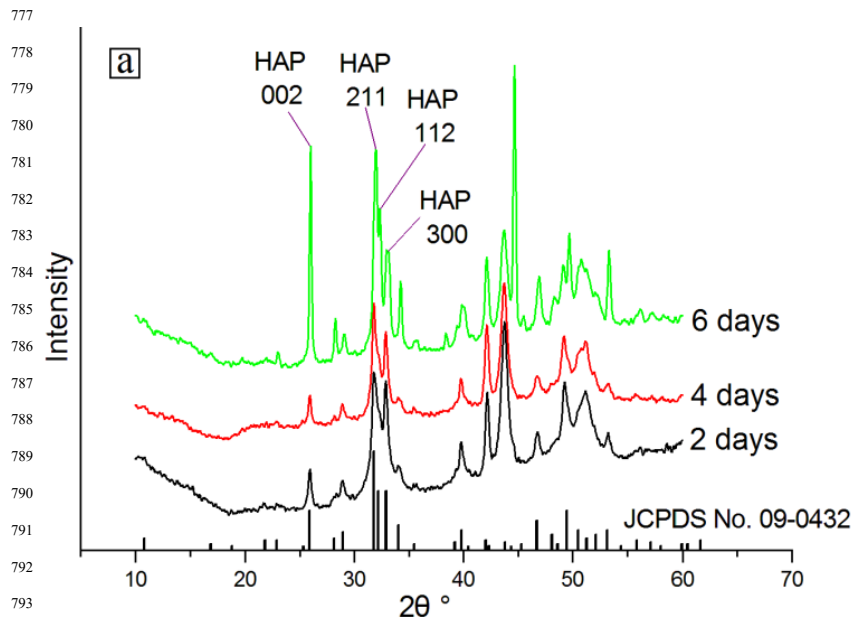
699
700
701
702
703
704
705
706
707
708
709
710
711
712
713
714
715
716
717
718
719
720
721
722
723
724
725
726
727



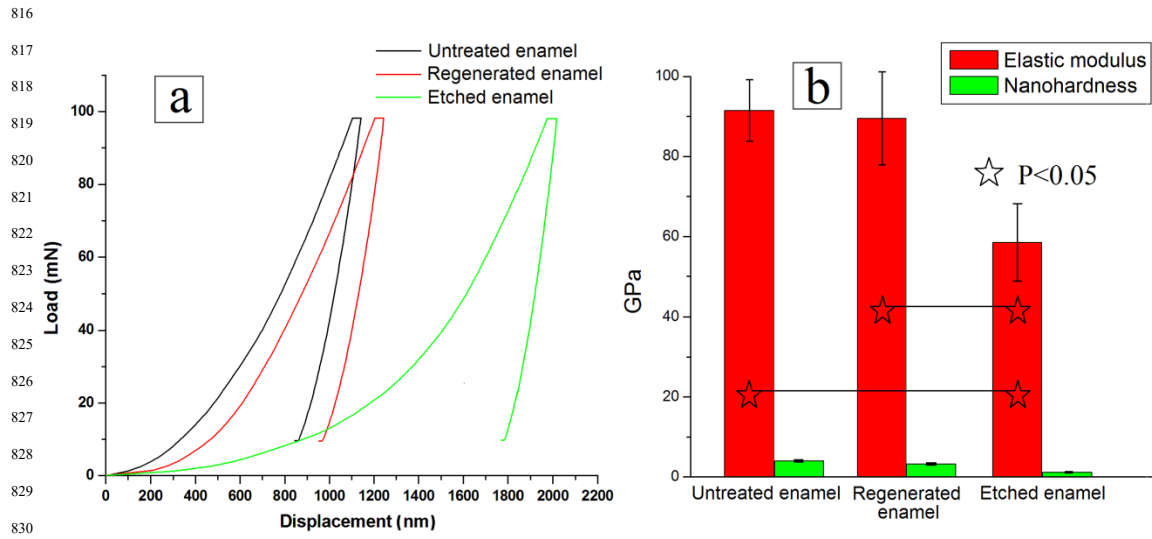
728 **Figure 5.** 3D AFM tapping-mode images of the etched enamel
729 and regenerated mineralised tissue. (a) Etched enamel. (b)
730 Regenerated mineralised tissue after 2 days. (c) Regenerated
731 mineralised tissue after 4 days. (d) Regenerated mineralised
732 tissue after 6 days.



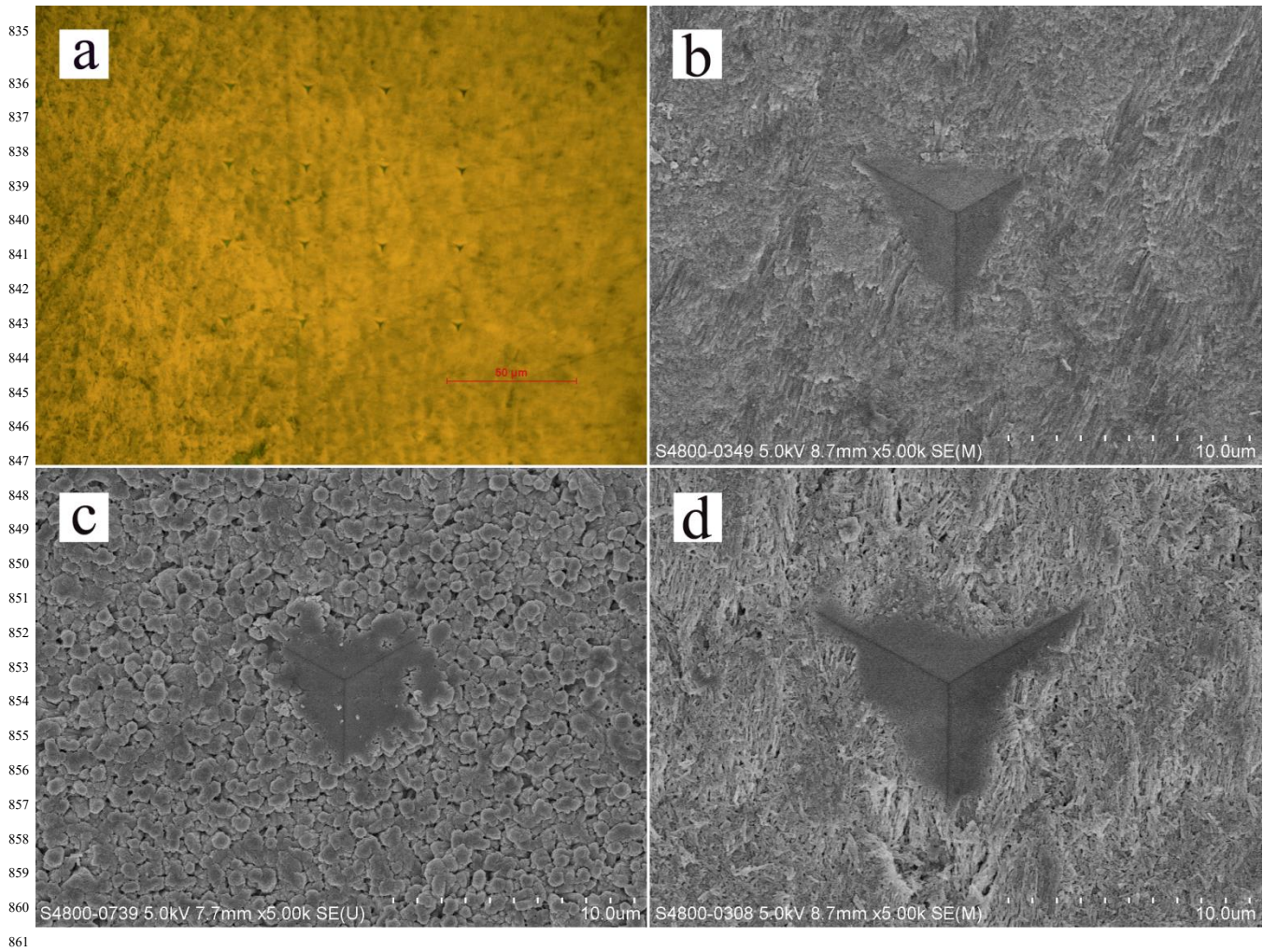
768 **Figure 6.** SEM and TEM micrographs of the replaced hydrogel
 769 after 2 days. (a) Polymer (agarose fiber)-mineral complex
 770 globules in the replaced CaCl₂ hydrogel. (b) Magnified
 771 micrograph of (a) to show the coalescence of nano-spheres.
 772 (c) TEM micrograph of the polymer (agarose fiber)-mineral
 773 complex globules. (d) SAED pattern of the mineral globule
 774 showing no evidence of reflective arcs. (e) A few globules in
 775 the replaced ion-free hydrogel. (f) Magnified micrograph of
 776 (e).



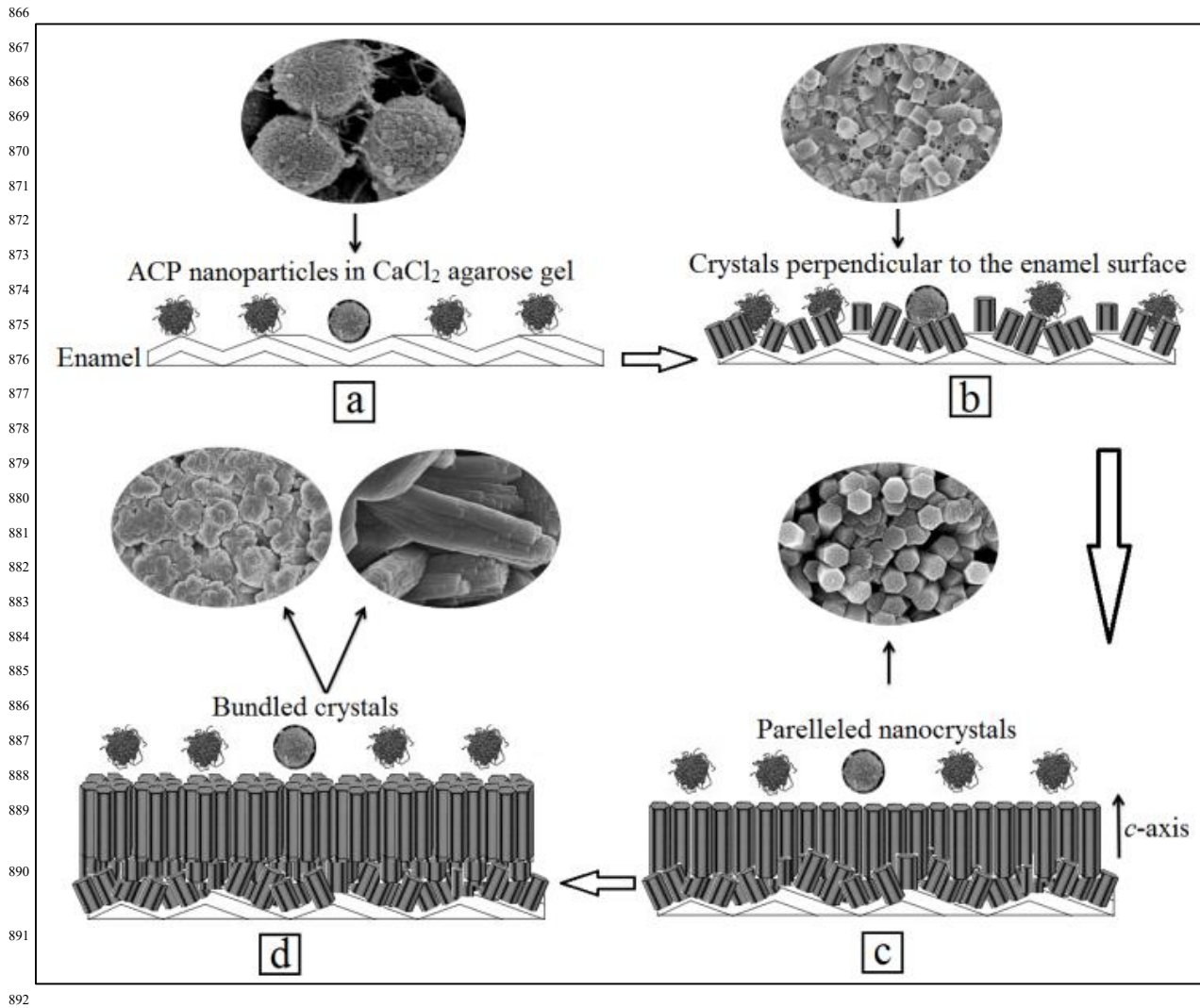
814 **Figure 7.** XRD (a) and FTIR (b) spectra of the regeneration layer
 815 on the enamel surface after 2, 4 and 6 days.



831 **Figure 8.** Typical Loading-unloading curves (a) and elastic
 832 modulus and nano-hardness (b) on the untreated,
 833 regenerated and acid-etched enamel after 6 days.



862 **Figure 9.** Optical microscope image of the regenerated
863 enamel surface with nano-indentations (a). SEM images of the
864 indentation impression on the surface of untreated enamel
865 (b), regenerated enamel (c) and etched enamel (d).



893 **Figure 10.** Schematic diagrams demonstrating the non-
894 classical crystallisation pathway. (a) ACP nanoparticles
895 nucleated on the lattice of the enamel HAP crystals. (b) The
896 initial precipitated crystals grew along its *c*-axis which is
897 perpendicular to the enamel prism surface. (c) Well-defined
898 hexagonal crystals were evenly distributed and densely
899 packed on the enamel surface. The mode of crystal growth
900 forced the rod crystals to align parallel to each other. (d) A
901 long, large hexagonal crystal acted as a primary crystal in the
902 center of the bundles, and short nanorods fused and aligned
903 parallel to the surface of the primary crystal to form enamel
904 prism-like structure.

905 AUTHOR INFORMATION

906 Corresponding Author

907 *E-mail: chchu@hku.hk (C.H. Chu); ql-li@126.com (Q.L. Li)

908 Tel: (+)852-28590287(C.H. Chu); (+)86-551-65118677(Q.L. Li)

909 Fax: (+)852-28587874(C.H. Chu); (+)86-551-65111538(Q.L. Li)

910 Notes

911 The authors declare no competing financial interest.

912 ACKNOWLEDGMENT

913 This study was supported by grants from the NSFC/RGC Joint
914 Research Scheme (N_HKU 776/10 and No.81061160511).

915 SUPPORTING INFORMATION

916 The crystals formed in the agarose hydrogel model
917 under different fluoride concentrations are
918 presented. This material is available free of charge via
919 the Internet at <http://pubs.acs.org>.

920 REFERENCES

921 1. Zhou, Y. Z.; Cao, Y.; Liu, W.; Chu, C. H.; Li, Q. L. *ACS Appl.*
922 *Mater. Interfaces*. **2012**, *4*, 6901-6910.

923 2. Cao, Y.; Liu, W.; Ning, T.; Mei, M. L.; Li, Q. L.; Lo, E. C.;
924 Chu, C. H. *Clin. Oral. Investig.* **2013**. [Epub ahead of print].

925 3. Chen, H. F.; Tang, Z. Y.; Liu, J.; Sun, K.; Chang, S. R.; Peters,
926 M. C.; Mansfield, J. F.; Czajka-Jakubowska, A.; Clarkson, B.
927 H. *Adv. Mater.* **2006**, *18*, 1846-1851.

928 4. Fincham, A. G.; Moradian-Oldak, J.; Simmer, J. P. *J. Struct.*
929 *Biol.* **1999**, *126*, 270-299.

930 5. Selwitz, R. H.; Ismail, A. I.; Pitts, N. B. *Lancet* **2007**, *369*,
931 51-59.

932 6. Zhan, J. H.; Tseng, Y. H.; Chan, J. C. C.; Mou, C. Y. *Adv.*
933 *Funct. Mater.* **2005**, *15*, 2005-2010.

934 7. Fowler, C. E.; Li, M.; Mann, S.; Margolis, H. C. *J. Mater.*
935 *Chem.* **2005**, *15*, 3317-3325.

936 8. Yamagishi, K.; Onuma, K.; Suzuki, T.; Okada, F.; Tagami,
937 J.; Otsuki, M.; Senawangse, P. *Nature* **2005**, *433*, 819.

938 9. Ye, W.; Wang, X. X. *Mater. Lett.* **2007**, *61*, 4062-4065.

939 10. Fan, Y.; Sun, Z.; Moradian-Oldak, J. *Biomaterials* **2009**,
940 *30*, 478-483.

941 11. Ruan, Q.; Zhang, Y.; Yang, X.; Nutt, S.; Moradian-Oldak,
942 J. *Acta. Biomater.* **2013**, *9*, 7289-7297.

943 12. Satoshi, S.; Shimokawa, H. In *Dental Enamel: Formation*
944 *to Destruction*. Robinson, C.; Kirkham, J.; Shore, R. Publisher:
945 CRC Press, **1995**; Ch. 4, p 87.

946 13. Busch, S. *Angew. Chemie*. **2004**, *43*, 1428-1431.

947 14. Silverman, L.; Boskey, A. L. *Calcif. Tissue Inter.* **2004**, *75*,
948 494-501.

949 15. Wei, J.; Wang, J. C.; Shan, W. P.; Liu, X. C.; Ma, J.; Liu, C.
950 S.; Fang, J.; Wei, S. C. *J. Mater. Sci-Mater. M.* **2011**, *22*, 1607-
951 1614.

952 16. Ungar, T. *Scripta. Mater.* **2004**, *51*, 777-781.

953 17. Chang, M. C.; Tanaka, J. *Biomaterials* **2002**, *23*, 4811-
954 4818.

955 18. Cha, C.; Kim, E. S.; Kim, I. W.; Kong, H. *Biomaterials* **2011**,
956 *32*, 2695-2703.

957 19. Moradian-Oldak, J.; Tan, J.; Fincham, A. G. *Biopolymers*
958 **1998**, *46*, 225-238.

959 20. Iijima, M.; Moriwaki, Y.; Wen, H. B.; Fincham, A. G.;
960 Moradian-Oldak, J. *J. Dent. Res.* **2002**, *81*, 69-73.

961 21. Wen, H. B.; Moradian-Oldak, J.; Fincham, A. G. *J. Dent.*
962 *Res.* **2000**, *79*, 1902-1906.

963 22. Iijima, M.; Moradian-Oldak, J. *Biomaterials* **2005**, *26*,
964 1595-1603.

965 23. Fan, Y. W.; Wen, Z. Z. T.; Liao, S. M.; Lallier, T.; Hagan, J.
966 L.; Twomley, J. T.; Zhang, J. F.; Sun, Z.; Xu, X. M. *J. Bioact.*
967 *Compat. Pol.* **2012**, *27*, 585-603.

968 24. Colfen, H.; Mann, S. *Angew. Chem.* **2003**, *42*, 2350-
969 2365.

970 25. Cao, Y.; Mei, M. L.; Xu, J.; Lo, E. C.; Li, Q.; Chu, C. H. *J.*
971 *Dent.* **2013**, *41*, 818-825.

972 26. Ning, T. Y.; Xu, X. H.; Zhu, L. F.; Zhu, X. P.; Chu, C. H.;
973 Liu, L. K.; Li, Q. L. *J. Biomed. Mater. Res. B.* **2012**, *100B*, 138-
974 144.

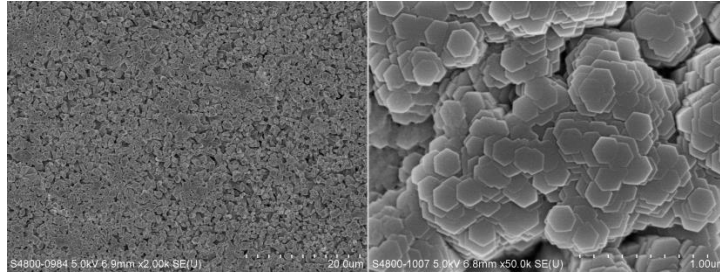
975 27. Gu, L. S.; Kim, Y. K.; Liu, Y.; Takahashi, K.; Arun, S.;
976 Wimmer, C. E.; Osorio, R.; Ling, J. Q.; Looney, S. W.; Pashley,
977 D. H.; Tay, F. R. *Acta. Biomater.* **2011**, *7*, 268-277.

978 28. Ge, J.; Cui, F. Z.; Wang, X. M.; Feng, H. L. *Biomaterials*
979 **2005**, *26*, 3333-3339.

980 29. Finke, M.; Hughes, J. A.; Parker, D. M.; Jandt, K. D. *Surf.*
981 *Sci.* **2001**, *491*(3), 456-467.

982 30. Habelitz, S.; Marshall, S. J.; Marshall, G. W., Jr.; Balooch,
983 M. *Arch. Oral. Biol.* **2001**, *46*, 173-183.

Table of Contents



Supporting information

Iijima et al(1) found the fluoride was crucial for the organized rod-like apatite crystal formation. In our experiment, we found that fluoride affected the morphology of the calcium phosphate crystals in the biomimetic mineralization of enamel.

In our agarose hydrogel model with phosphate solution containing 500ppm fluoride, hexagonal rod crystals were formed after 6 days of incubation (Figure 2, 3, 4). Enamel prism-like bundles consisted of aggregated rod crystals were found (Figure 4). When the fluoride concentration was reduced to 100ppm, ribbon-like crystal was formed (Figure S1), and they consisted of paralleled needle-like crystals (Figure S1b Arrow). In the absence of fluoride, plate-like crystals were found on the enamel surface (Figure S2). Enamel has a high packing density of apatite crystals but the precipitated plate-like and ribbon-like apatite layer was a loose aggregate of the crystals with a porous structure. The layer formed with plate-like or ribbon-like crystals thus could not offer any mechanical function of hard tissues.

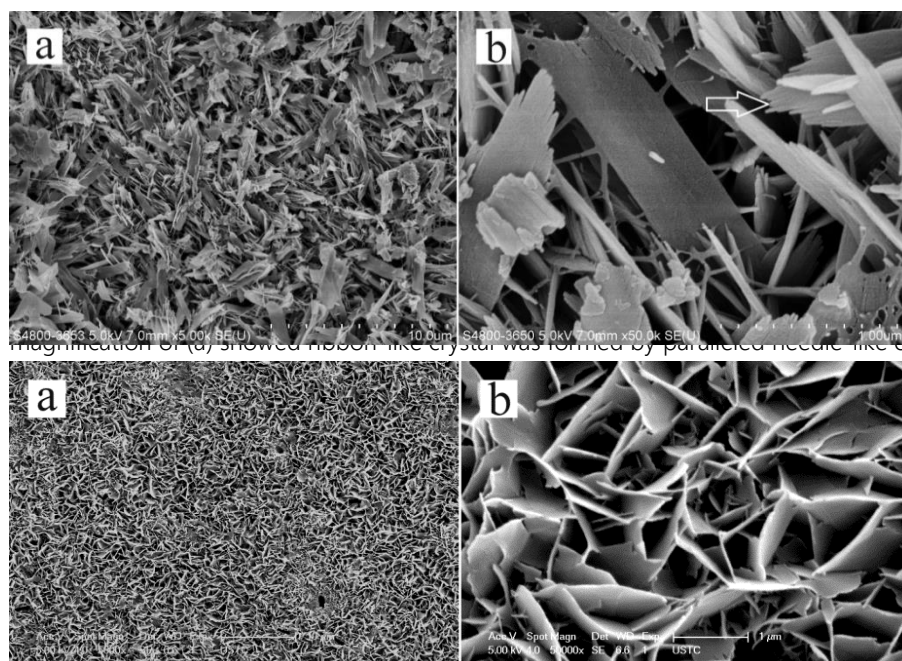


Figure S2. (a) Plate-like crystals regenerated on the enamel surface without fluoride after 4 days. (b) High-magnification of (a) showed ribbon-like crystal was formed by paralleled needle-like crystals. (c) High-magnification of (c) showed ribbon-like crystal was formed by paralleled needle-like crystals.

Figure S2. (a) Plate-like crystals regenerated on the enamel surface without fluoride after 4 days. (b) High-magnification of (a) showed ribbon-like crystal was formed by paralleled needle-like crystals. (c) High-magnification of (c) showed ribbon-like crystal was formed by paralleled needle-like crystals.

References:

1. Iijima, M.; Moradian-Oldak, J., Control of apatite crystal growth in a fluoride containing amelogenin-rich matrix. *Biomaterials* **2005**, 26 (13), 1595-603.

Reviewer's comment	Authors' response
<p>Reviewer #1: Recommendation: Do not publish.</p> <p>Comments: There is nothing new in this report and the data are poorly interpreted. The study mostly repeats what has been already done using slightly different experimental setting and different gel. The authors used calcium containing agarose-based gel to remineralize etched enamel surfaces. Electron microscopy, XRD and FTIR were used to characterize the composition of the product. Mechanical properties were accessed by Berkovith nanoindentation tip.</p> <p>General Concerns to be addressed: The strategy used in this report is very similar to what has already been reported by other investigators using gelatin (Busch et al 2004), agarose (Fan et al 2012), and recently chitosan-amelogenin (Ruan et al 2013).</p>	<p>Regeneration of enamel structure with acellular method is an important field of study in biomaterial science and dentistry. Studies so far demonstrated success in partially mimicking the assembly steps of enamel crystals and enamel-like structure formation. However, there is no study (including the articles suggested by the reviewer) can demonstrate regeneration of enamel microstructure. Therefore, it is essential to develop model for enamel regeneration.</p> <p>Our study is unique because:</p> <p>1) Busch et al. Regeneration of human tooth enamel. <i>Angew. Chem. Int. Ed.</i> 2004;43:1428-31. Busch et al. used gelatine hydrogel for regeneration of enamel-like mineral, but we used agarose. The agarose used in our model is not a simple replacement of materials, the mechanism is also different. The specialty and advantages are discussed in our paper (page 1 lines 68-76, page 4 lines 390-395, 398-411, marked in red).</p> <p>2) Fan et al. Novel amelogenin-releasing hydrogel for remineralization of enamel artificial caries. <i>J Bioact & Compat Polym</i> 2012;27:585-603. Fan et al used agarose as a releasing agent to study the function of amelogenin in remineralization. In the absence of amelogenin, they did not show the regeneration of enamel-like structure. We constructed a model using agarose without cell and/or protein for enamel remineralization. The aim and function of the use of agarose by Fan et al are different from those by our study and theirs. Therefore, the two studies cannot be compared. This is discussed in page 4 lines 412-423, marked in blue.</p>

<p>The development of fluorapatite cement for dental enamel defect has been also reported lately (fluorapatite cement (Wei et al 2011).</p> <p>This is also too similar to what has been reported in 2006 by Chen et al.</p> <p>The experimental procedures lack details and there are problems with the data and their interpretation.</p> <p>Based on the morphology and size of the crystals, it appears that the authors grew fluorapatite and not hydroxyapatite.</p> <p>The mechanical testing was performed only on one sample with nine points and this is not adequate for statistical analysis. At least three different samples for each need to be tested.</p> <p>For specific comments see below: Title: The word “Novel” is overused in the title.</p>	<p>3) Ruan et al. An amelogenin-chitosan matrix promotes assembly of an enamel-like layer with a dense interface. <i>Acta Biomaterialia</i>. 2013;9: 7289-97. Ruan et al developed an amelogenin-containing chitosan hydrogel for enamel reconstruction. Ruan et al used amelogenin, but we used an agarose model with no amelogenin to regenerate enamel-like tissue. This is discussed in page 4 lines 423-432, marked in red.</p> <p>Wei et al. Development of fluorapatite cement for dental enamel defects repair. <i>J Mater Sci: Mater Med</i>. 2011; 22:1607-1604. Wei et al used apatite cement pastes to fill enamel defects. We used a biomimetic mineralization model to induce enamel-like tissue formation, and the prospective application of our model will be different from their study. This is discussed in page 6 lines 581-587, marked in red.</p> <p>Chen et al. Acellular Synthesis of a Human Enamel-like Microstructure. <i>Adv. Mater</i>.2006; 18:1846-1851. Chen et al used a hydrothermal technique (121°C) on various substrate plates, such as iron and titanium, to produce enamel-like tissue. The theory, conditions and prospective application of hydrothermal technique are different from our study method. This is discussed page 1 lines 42-50, marked in red.</p> <p>Further information was added (page 2 lines 98-108, marked in red).</p> <p>Agree. The regenerated crystals were fluoridated hydroxyapatite. This was amended in page 3 lines 279-284, marked in red.</p> <p>We performed the mechanical test using 3 samples with a total of 144 points as suggested by the reviewer. This is added in Method (page 2 lines 161-162, 180-183, 190-193) and in Results (page 3 lines 327-328, marked in blue) and Figure 9.</p>
--	---

<p>The novelty of using agarose gel in enamel remineralization is questionable. See Fan et al 2012, in Bioactive and Compatible Polymers</p> <p>It is not clear what makes this strategy “biomimetic”??</p> <p>Is this a “gel” or “hydrogel”?? Both terms are used throughout the text for agarose.</p> <p>What is the concentration??</p> <p>Introduction: The notion that electro deposition system was done at 85 c degree in the presence of amelogenin is wrong.</p> <p>What is the advantage of agarose over gelatin and other gels??</p> <p>Materials and Methods The experimental details for calcium and phosphate concentration as well as agarose concentration are missing.</p> <p>Results and Figures: Section 3.1 and Fig 2 can be removed since it does not add any new information and similar findings have already been reported in the literature.</p> <p>Figure 3: There is no indication that the crystals are aligned parallel to each other.</p> <p>In the presence of 500ppm F those hexagonal prisms cannot be HAP but they are fluorapatite crystals.</p>	<p>The title is amended. The word “Novel” is replaced by “agarose”.</p> <p>The difference between our study and Fan et al 2012 was discussed (page 4 lines 412-423, marked in blue).</p> <p>We use agarose hydrogel to mimic the gel-like micro-environment during enamel formation. The hydrogel also maintains a unidirectional Ca^{2+} and PO_4^{3-} supply. Moreover, our study was performed at 37°C, but not at high temperature or at high pressure. This is discussed in page 4 lines 363-379, marked in blue.</p> <p>Done. The ‘gel’ is changed to “hydrogel”.</p> <p>The concentration is 0.5%. This is added in page 2 lines 98-103, marked in red.</p> <p>Amended. The reference should be Ye et al 2007 (page 1 lines 47-48 and page 16 line 954, marked in red).</p> <p>The advantage of agarose over gelatin and other gels is added in page 1 lines 68-76, page 4 lines 390-395, marked in red.</p> <p>Done. The details are added in page 2 lines 98-108, marked in red.</p> <p>Done. Section 3.1 and Fig 2 are removed.</p> <p>Agree. The crystals were perpendicular to the enamel prism (page 2 lines 201-211, marked in blue and Figure 2).</p> <p>Agree. The regenerated crystals were fluoridated hydroxyapatite (page 3 lines 279-284, marked in red).</p>
---	--

<p>Figure 4”” these structures are not typical to enamel crystals. The authors are encouraged to look at some literature for the morphology of enamel crystals.</p> <p>Figure 5: What is the relation between C and d??</p> <p>Figure 6: The TEM in f is not crystalline while the claim for b and e states that they are crystalline. It is not clear what the authors want to convey with showing this figure??</p> <p>Figure 7: The XRD pattern is indicative of fluorapatite (FA) (see Jie Wei et al , J Mater Sci 22, 1607, 2011, Chen et al 2006 in the reference list).</p> <p>The FTIR is not detailed enough to distinguish between FA and HAP.</p> <p>Figure 8: The results of Fig 8b is very surprising because the elastic modulus of the regenerated enamel is unusually high and similar to enamel.</p> <p>The use of one sample for these mechanical testing is not enough and at least three samples of each needs to be tested and averaged. Nine points on each sample is also minimal.</p> <p>It is not clear what figure 10 is based on??</p> <p>What is the base of classical crystallization pathway?? As oppose to n</p>	<p>The crystals (Figure 3) are intermediates during the crystal self-assembly. Certain rod crystals self-assemble together to form the rudiment of enamel prism-like bundles (Figure 3b highlighted in Oval). This is added in page 3 lines 221-223 and discussed in page 5 lines 528-534, marked in red.</p> <p>In Figure 4, 4c (bundle surface) and 4d (side view of the bundle) are images at high magnifications from 4a. (Page 9 lines 699-703, marked in red).</p> <p>Figure 6b and 6d suggests an amorphous structure. This is added in page 3 lines 267-275, marked in blue.</p> <p>Agree. The result is amended (page 3 lines 279-284, marked in red). The two references are added in page 16 lines 940-942, 965-967, marked in red.</p> <p>Agree. This is added in page 3 lines 304-310, marked in red.</p> <p>The elastic modulus of the regenerated tissue was comparable to those of the untreated enamel surface, probably due to their similar microstructures. Similar results were also reported by <i>Busch et al (2004)</i>. This is discussed in page 5 lines 571-579, marked in blue.</p> <p>Agree. 144 points of indentations from 3 samples were performed. This is added in Method (page 2 lines 161-162, 180-183, 190-193), Results (page 3 lines 327-328, marked in blue) and Figure 9.</p> <p>Figure 10 illustrates the process of the enamel prism-like crystals growth in our study. It is based on our findings, especially the SEM observations and referring to the mechanism of non-classical crystallization pathway. This is discussed in Discussion 4.2 (page 4 lines 440-457, page 5 lines 468-493, 539-543, marked in blue).</p>
---	---

<p>Additional Questions:</p> <p>Is this paper in the top 20% of manuscripts in the field?: No</p> <p>If this paper is not in the top 20% of manuscripts in the field: It is unlikely to be improved to be in the top 20%.</p> <p>Is it appealing to a broad audience?: No</p> <p>Does the manuscript give a complete description of the procedures that could be reproduced by others in the field?: No</p> <p>Are the literature references appropriate and up to date?: Yes</p> <p>Provides significant insight into or the development of an important application: Poor</p> <p>Work is original and significant: Poor</p> <p>Conclusions adequately supported by data: Poor</p> <p>Clarity of presentation: Fair</p> <p>Potential for impact in materials science and engineering: Fair</p>	<p>Classical crystallization pathway is thermodynamic process where ion-mediated crystallization proceeds via a one-step route to the final mineral phase. Non-classical crystallization pathway is a kinetic process where crystallization proceeds by a sequential process involving structural and compositional modifications of amorphous precursors and crystalline intermediates. (Page 4 lines 440-446, marked in blue).</p>
---	--

Reviewer's comment	Authors' response
<p>Reviewer #2: Recommendation: Publish after revisions noted.</p> <p>Comments: The authors present interesting data in regenerating enamel prism-like structure through a novel hydrogel biomimetic model. The study is well-designed and the paper is well written. The reviewer would suggest publication after its revision suggested below.</p> <p>In details:</p> <p>1. In the agarose gel model, in addition to the Ca and Phosphate sources, a sodium fluoride solution has been added to the system.</p> <p>What is the role of F⁻ in the synthesis of HAP crystals?</p> <p>Any fluorapatite or fluor-hydroxyapatite formation? Please provide experimental data and discuss.</p> <p>2. Please show and discuss how this biomimetic model would be transferred for future clinical applications.</p> <p>How the saliva containing oral environment affect the synthesis of HAP crystals?</p> <p>How is this model going to target the common enamel subsurface lesions?</p> <p>3. There is a lack of details in the preparation of this agarose gel system, which should be provided for the repetition of the experiment.</p>	<p>The authors appreciate the reviewer's encouraging comments.</p> <p>Experiment of the effects of concentration of fluoride on crystal regeneration is provided as supporting information (page 5 lines 459-466, page 16 lines 929-933, marked in red).</p> <p>The role of fluoride was discussed in the supporting information (page 16 lines 929-933, marked in red).</p> <p>Yes. The crystals formed were fluoridated hydroxyapatite (page 3 lines 279-284, 304-310, marked in red). Experiment of the effects of concentration of fluoride on crystal regeneration is provided as supporting information (page 5 lines 459-466, marked in red) and discussed in the supporting information (page 16 lines 929-933, marked in red).</p> <p>Further information was added in Discussion (page 6 lines 598-602, marked in blue).</p> <p>Further information was added in Discussion (page 6 lines 606-608, marked in blue).</p> <p>Further information was added in Discussion (page 6 lines 602-605, marked in red).</p> <p>Done This is added in page 2 lines 98-108, marked in red).</p>

<p>4. The authors should explain the mechanisms of the breakdown of agarose matrix while the HAP crystals are undergoing maturation process.</p> <p>Additional Questions:</p> <p>Is this paper in the top 20% of manuscripts in the field?:</p> <p>If this paper is not in the top 20% of manuscripts in the field:</p> <p>Is it appealing to a broad audience?: No</p> <p>Does the manuscript give a complete description of the procedures that could be reproduced by others in the field?: No</p> <p>Are the literature references appropriate and up to date?: Yes</p> <p>Provides significant insight into or the development of an important application: Good</p> <p>Work is original and significant: Good</p> <p>Conclusions adequately supported by data: Good</p> <p>Clarity of presentation: Good</p> <p>Potential for impact in materials science and engineering: Fair</p>	<p>The mechanism of the breakdown of agarose matrix was discussed in page 5 lines 508-520, marked in red.</p>
---	---

Reviewer's comment	Authors' response
<p>Reviewer #3: Recommendation: Publish after revisions noted.</p> <p>Comments:</p> <p>This manuscript describes a novel hydrogel biomimetic mineralization model for the regeneration of enamel prism-like tissue. SEM, TEM, XRD, FTIR and the nano-indentation hardness test have been used for analyzing the physicochemical properties of the regeneration enamel and the agarose.</p> <p>Whereas, for reliable surface characterization, parameters describing surface variation in the spatial direction are additionally needed, so I would consider adding the 3D surface analyze by using AFM. The results showed that this novel hydrogel biomimetic mineralization model is useful for the regeneration of enamel prism-like tissue.</p> <p>Overall, the paper is well written, well organized. The topic and results of this study are interesting. I would recommend this manuscript for publication in ACS Applied Materials & Interfaces, provided the authors reasonably address the following points.</p> <p>The following are concerns that should be deliberated in the paper:</p> <ol style="list-style-type: none"> 1. The tooth slices were covered with nail vanishes. What is the purpose of using nail vanishes and which kind of nail vanishes was used? 2. Which kind of statistics analysis was used for elastic modulus and nanohardness test (Figure 8b)? 3. "The regenerated crystals on the enamel surface formed a homogenous and dense layer of mineralized tissue after 6 days of incubation. 	<p>3D surface analysis by using AFM was performed as suggested by the reviewer. This is added in Figure 5 and page 2 lines 131-132, 134-136, page 3 lines 251-265, marked in red.</p> <p>The authors appreciate the reviewer's encouraging comments.</p> <p>The nail vanish was used to protect the enamel surface from treatment such as etching and subsequent remineralisation, so that they can be used as control for comparison. Further information was added in page 2 lines 152-156, marked in red.</p> <p>Two-way ANOVA was used (page 2 lines 190-193, marked in blue).</p> <p>Amended. We redid the mechanical test using 3 samples after 6 days of incubation. Further information was added in page 2 lines 161-162,</p>

<p>“But in evaluation of mechanical properties, the tooth slices were incubated for 4 days.</p> <p>4. The magnification of SEM micrographs was not unified. Etched human enamel was used as control but the magnification of SEM micrographs of etched human enamel (Figure 2) was not the same as SEM micrographs of the regenerated mineralized tissue after 2,4 and 6 days (Figure 3,4 and 5).</p> <p>Why it didn't have SEM micrographs of c-axis and cross-sectional view after 4 days (Figure 4)?</p> <p>5. Did the diameter of rod crystals changed over time?</p> <p>As shown in Figure3c and Figure4b, the diameter of rod crystals was expressed remarkably different with the same magnification. If it changed, what the reason it is? If it not changed, why looked different in same magnification?</p> <p>6. I would like to see the experiments using this regenerated enamel in vitro study.</p> <p>Additional Questions: Is this paper in the top 20% of manuscripts in the field?: No</p> <p>If this paper is not in the top 20% of manuscripts in the field: It could be improved to be in the top 20% with appropriate revisions.</p> <p>Is it appealing to a broad audience?: Yes</p> <p>Does the manuscript give a complete description of the procedures that could be reproduced by others in the field?: Yes</p> <p>Are the literature references appropriate and up to date?: Yes</p> <p>Provides significant insight into or the development of an important application: Good</p>	<p>180-183, 190-193, page 4 lines 327-328, marked in blue. Figure 9 was amended.</p> <p>SEM micrographs were unified now.</p> <p>SEM micrographs of c-axis and cross-sectional view after 4 days are added (Figure 3).</p> <p>Yes. The diameter of rod crystals changed over time.</p> <p>The reason was discussed in page 5 lines 508-520, marked in red.</p> <p>This model is an in vitro study. We plan to do in vivo study in near future.</p>
--	--

Work is original and significant: Good	
Conclusions adequately supported by data: Good	
Clarity of presentation: Good	
Potential for impact in materials science and engineering: Good	

Editor's comment	Authors' response
<p>On the basis of the reviewer comments and my own assessment of the manuscript, I am willing to consider a revised version of this paper for publication in ACS Applied Materials & Interfaces pending a second round of external review.</p> <p>In preparing the revision, carefully consider all of the comments made by the reviewers. In particular, you must address the novelty issues of this work raised by Reviewer 1.</p> <p>We would like to receive your revision as soon as possible, by 03-Dec-2013 at the latest.</p> <p>In addition to addressing the reviewers' comments, please make each of the technical corrections listed below:</p> <p>1) For the benefit of reviewers during the second round of external review, you must incorporate/include all your responses to reviewer comment directly into the revised manuscript, and not just in the Response Letter. In your Response Letter, you must also indicate the page and line number in the manuscript where your responses/corrections have been incorporated</p> <p>2) NEED new Journal Publishing Agreement. Please go to your Paragon Plus website and click the link "Forms to be completed" and follow the instructions to submit the electronic journal publishing agreement form.</p> <p>a) As your JPA was addressed to Chemistry of Materials, we would like to know if this manuscript was previously submitted to Chemistry of Materials and the outcome of previous submission.</p> <p>3) Supporting Information (SI): If needed in the revised manuscript, a Supporting Information paragraph should be included after the acknowledgment paragraph. The paragraph should describe the contents of the SI section, and the last line should read as follows: "This information is</p>	<p>Done. A point to point response is made.</p> <p>We have asked for extension of the due date to 31 Dec 2013 and have been approved.</p> <p>Done. A point to point response is made and amendment in response or as suggested by the reviewers are made accordingly in the manuscript. These amendments are highlighted for reference by the reviewers in the revised manuscript submitted as supporting document.</p> <p>Done.</p> <p>This manuscript was submitted to Chemistry of Materials, and the editor of Chemistry of Materials considered it more suitable for journal that specializes in applied materials or biomedical materials.</p> <p>Done.</p>

<p>available free of charge via the Internet at http://pubs.acs.org/.</p> <p>4) Reference Formatting: The references are not formatted according to journal standard. See the journal at http://pubs.acs.org/journal/aamick for example of proper format.</p> <p>a) Use CASSI abbreviations for all journal names. See http://www.cas.org/sent.html for list of journal name abbreviations.</p> <p>b) All Refs missing end page numbers; Ref 2 missing volume and page numbers, not found on CASSI ; Ref 12 incomplete reference; Ref 13,15,23 incorrect journal name abbreviation; Ref 27 journal name not abbreviated</p> <p>5) Figures and tables need to be reformatted.</p> <p>a) Axis labels and tick markers in figures/plots are too small. Increase font sized used.</p> <p>b) Please provide error limits on data in tables/plots.</p> <p>c) Figure 10 missing labels in caption</p> <p>6) On resubmission, please provide 2 copies of the final manuscript file:</p> <p>a) The final revised manuscript file that does not contain any highlighting or editing marks. This file should be uploaded as the primary manuscript document file.</p> <p>b) A marked copy of the revised manuscript that shows changes made on revision clearly highlighted. This file should be uploaded SEPARATELY FROM THE FINAL MANUSCRIPT FILE as Supporting Information for Review.</p> <p>Do not add any highlighting or other editing marks to the supporting information file that is intended to be published with the manuscript (this file is uploaded as "supporting information for publication").</p>	<p>Done.</p> <p>Done.</p> <p>Amended. (Ref 2, 12, 13, 16, 26 and 29 are highlighted in blue in page16, 17)</p> <p>Done.</p> <p>Done.</p> <p>Done.</p> <p>Done.</p> <p>Done.</p> <p>Done.</p>
--	--

